

## Crossover from fragile to strong glassy behaviour in the spin facilitated chain model

This article has been downloaded from IOPscience. Please scroll down to see the full text article.

2002 J. Phys.: Condens. Matter 14 1499

(<http://iopscience.iop.org/0953-8984/14/7/308>)

View [the table of contents for this issue](#), or go to the [journal homepage](#) for more

Download details:

IP Address: 171.66.16.27

The article was downloaded on 17/05/2010 at 06:09

Please note that [terms and conditions apply](#).

# Crossover from fragile to strong glassy behaviour in the spin facilitated chain model

Arnaud Buhot and Juan P Garrahan

Theoretical Physics, University of Oxford, 1 Keble Road, Oxford OX1 3NP, UK

Received 3 December 2001

Published 7 February 2002

Online at [stacks.iop.org/JPhysCM/14/1499](http://stacks.iop.org/JPhysCM/14/1499)

## Abstract

We discuss equilibrium and out-of-equilibrium dynamical properties of the spin facilitated chain model. The two well known limiting cases of full asymmetry and symmetry of the dynamical rules respectively lead to pure fragile and strong glassy behaviours. A crossover from fragile to strong glassy behaviour at a finite temperature exists for a large asymmetry. The tunable asymmetry, which plays the role of an entropic barrier, allows the crossover temperature to be controlled. Analytical predictions are confirmed by numerical simulations.

## 1. Introduction

The glass phase is as common in nature as the gas, liquid or solid ones. Most liquids, when cooled sufficiently rapidly, avoid crystallization to form an amorphous, microscopically disordered solid called a glass. Yet the dynamical behaviour of glasses is not well understood, especially the relaxation time (or the viscosity) which increases by several orders of magnitude when the temperature is lowered. Several years ago, Angell [1] proposed a classification of glasses in terms of the shape of the logarithm of this relaxation time plotted against the inverse temperature. Strong glasses are characterized by a linear behaviour or an Arrhenius law and fragile ones by a highly nonlinear behaviour. Covalent glasses like  $\text{SiO}_2$  are prototypes for strong glasses whereas polymers or complex molecules are prototypes for fragile ones; however, some molecules like water fail to find a place in this classification, behaving as a fragile glass just below the glass temperature and as a strong one for low temperatures [2, 3].

In this paper we will show that the combination of two relaxation mechanisms, one with growing energy barriers and the other with a single energy barrier but also an entropic one, may lead to this crossover from fragile to strong glassy behaviour when the temperature is lowered. The entropic barrier, tunable with the asymmetry of the dynamical rules, determines the crossover temperature. The fragile mechanism leads to a stretched exponential relaxation with a temperature-dependent stretching exponent.

The paper is organized as follows: in section 2 we present the model and the dynamical rules and we define our notations. In section 3 the relevant timescales are discussed for the two different relaxation mechanisms. The crossover temperature is predicted. Some equilibrium

properties are presented in section 4 and out-of-equilibrium ones in section 5. In each case, numerical simulations confirm the analytical predictions. We conclude and discuss some extension of the model in section 6.

## 2. Model

In the following, we consider the 1D spin facilitated model which has been introduced by Fredrickson and Andersen [4] in its symmetric version and by Jäckle and Eisinger [5] in its asymmetric version. Both models are based on the same Hamiltonian  $H = \sum_i s_i$  of  $N$  non-interacting Ising spins  $s_i = 0, 1$  in a uniform magnetic field  $h = -1$ . The thermodynamical properties are trivial as a consequence of the non-interacting variables. For example, the equilibrium energy (which is also the concentration of 1-spins or *defects*) is given by  $c_{\text{eq}} = 1/[1 + \exp(1/T)]$ , with  $T$  the temperature. Despite the trivial equilibrium properties, interesting dynamical behaviour may be obtained by introducing constraints on the flipping rates of the spins. The general constraint for the probability  $P(s_i)$  to flip the spin  $s_i$ , which interpolates between the purely asymmetric and the symmetric models, is realized with [6]

$$P(s_i) = P_{\text{metro}}(\delta E) [b s_{i-1} + (1 - b) s_{i+1}] \quad (1)$$

where  $\delta E = 1 - 2s_i$  is the energy difference between final and initial configurations.  $P_{\text{metro}}(\delta E) = \min(1, \exp(-\delta E/T))$  is the usual Metropolis probability (Glauber or heat bath dynamics would lead to the same results). The second term of  $P(s_i)$  in equation (1) sets the constraints and imposes the presence of a neighbouring defect to facilitate the flip of the spin  $s_i$ .  $b$  is a free asymmetry parameter which allows different kinds of glassy behaviour. The two limiting cases  $b = 0$  (or equivalently  $b = 1$ ) and  $b = 1/2$  have been thoroughly studied [4–9]. The case  $b = 1/2$  corresponds to the symmetric one where the spin  $s_i$  needs a defect as a neighbour (irrespective of its position, left or right) to flip and leads to ‘strong glass’ behaviour [4]. The case  $b = 0$  corresponds to the fully asymmetric constraint where the spin  $s_i$  needs a neighbour on its right to flip [5]. As we shall see, a coarsening process with increasing energy barriers leads to fragile glass behaviour in this case [7]. The more interesting situation corresponds to intermediate values of  $b$  ( $0 < b < 1/2$ ) [10]. The asymmetry between left and right neighbours models an entropic barrier. In this case both symmetric and asymmetric relaxation processes are available and compete, leading to a crossover from fragile to strong glass behaviour.

## 3. Relevant timescales

Let us now describe the two relevant processes and corresponding timescales in the symmetric and fully asymmetric cases before considering the intermediate case  $0 < b < 1/2$ .

### 3.1. Symmetric dynamical rules: $b = 1/2$

In the symmetric case, two different timescales  $\tau_0$  and  $\tau_1$  are involved for the relaxation of a defect (at equilibrium). If one of the neighbours is also a defect, the spin  $s_i$  relaxes easily and the corresponding timescale is the microscopic one  $\tau_0 \sim 1$ , independently of the temperature. If the defect is isolated (without any neighbouring defects) two possible relaxation processes may occur using successively right and left neighbour defects (or vice versa)

$$010 \rightarrow 110 \rightarrow 100 \quad (2)$$

$$010 \rightarrow 011 \rightarrow 001. \quad (3)$$

These processes correspond to the motion of the isolated defect with a diffusion rate  $\Gamma \sim e^{-1/T}$  (due to the intermediate creation of a new defect). Thus the corresponding timescale  $\tau_1 = 1/\Gamma \sim e^{1/T}$ . The relaxation time, the largest of the two times  $\tau_0$  and  $\tau_1$ , follows an Arrhenius law typical of a strong glass with an energy barrier  $\Delta E = 1$

$$\tau_S \sim e^{\Delta E/T} = e^{1/T}. \quad (4)$$

### 3.2. Fully asymmetric dynamical rules: $b = 0$

In the purely asymmetric case, the dynamical constraints are maximal and only right neighbours may facilitate the evolution of a spin. As a consequence, the symmetric process involving both left and right neighbour defects is no longer available. In fact, it is possible to show that different timescales  $\tau_n$  appear for the relaxation of a defect depending on the length  $l$  of the chain of spins 0 on its right. For a length  $l = 0$  the right neighbour is also a defect and there is no dynamical constraint. The timescale  $\tau_0 \sim 1$  is independent of the temperature. For a length  $l = 1$  the timescale is  $\tau_1 \sim e^{1/T}$  and corresponds to the following process

$$101 \rightarrow 111 \rightarrow 011 \rightarrow 001 \quad (5)$$

involving an energy barrier  $\Delta E = 1$ .

More generally, for a length  $l$  with  $2^{k-1} \leq l < 2^k$ , the system has to overcome an energy barrier  $\Delta E = k$  to relax the defect and thus the corresponding timescale is  $\tau_k \sim e^{k/T}$  [7]. It is easy to understand why energy barriers only grow logarithmically with the length  $l$  from the relaxation process corresponding to a length  $l = 3$

$$\begin{aligned} 10001 &\rightarrow 10011 \rightarrow 10111 \rightarrow 10101 \rightarrow 11101 \\ 00001 &\leftarrow 00011 \leftarrow 00111 \leftarrow 00101 \leftarrow 01101 \leftrightarrow \end{aligned} \quad (6)$$

which overcomes an energy barrier of  $k = 2$ .

As we have seen, the timescale to flip a defect depends on the distance to the next defect on its right. In equilibrium, the average distance between defects is  $l_{\text{eq}} = 1/c_{\text{eq}} \sim e^{1/T}$ . Using this typical length we obtain the following relaxation time [7]

$$\tau_{\text{AS}} \sim \exp\left(\frac{\ln l_{\text{eq}}}{T \ln 2}\right) = e^{A/T^2} \quad (7)$$

with  $A = 1/\ln 2$ .

The timescale  $\tau_{\text{AS}}$  displays an exponential inverse temperature squared behaviour (or Bässler law behaviour [11]) characteristic of a fragile glass and used as an alternative to the Vogel–Fulcher law [12, 13]. The same timescale will be recovered later when discussing the persistence functions.

### 3.3. Asymmetric dynamical rules: $0 < b < 1/2$

The symmetric and fully asymmetric processes compete in the intermediate case. The symmetric process is constrained by the small value of the asymmetry parameter  $b$  and the diffusion rate  $\Gamma$  is modified accordingly ( $\Gamma \sim b(1-b)e^{-1/T}$ ) leading to

$$\tau_S(b) \sim e^{1/T} [b(1-b)]^{-1} = e^{\Delta E/T + \Delta S} \quad (8)$$

with the energy barrier  $\Delta E = 1$  and an entropic barrier  $\Delta S = -\ln[b(1-b)]$  coming from the asymmetry parameter. Assuming additivity of the rates we deduce the following relaxation time

$$\tau_I(T, b) = (\tau_{\text{AS}}^{-1} + \tau_S^{-1}(b))^{-1}. \quad (9)$$

For high temperatures the asymmetric process dominates due to the entropic barrier in the symmetric timescale. For low temperatures the symmetric process becomes dominant due to the fragile behaviour of the asymmetric timescale. The crossover temperature

$$T_c(b) \simeq \frac{\sqrt{1 + 4\Delta S / \ln 2} - 1}{2\Delta S} \quad (10)$$

corresponds to  $\tau_S(b) = \tau_{AS}$  and depends on the asymmetry parameter through the entropic barrier.

#### 4. Equilibrium properties

Due to the non-interacting variables, equilibrium properties are known exactly and as a consequence we are able to explicitly construct low-temperature equilibrium configurations. This allows us to study numerically the equilibrium dynamics down to really low temperatures in contrast with most of other glassy systems where only out of equilibrium quantities are accessible.<sup>1</sup>

##### 4.1. Correlation functions and relaxation time

The relaxation time  $\tau$  may be extracted from the equilibrium correlation function (normalized to  $[0, 1]$ ):

$$C_{\text{eq}}(t) = \frac{\langle s_i(t)s_i(0) \rangle - c_{\text{eq}}^2}{c_{\text{eq}} - c_{\text{eq}}^2} \quad (11)$$

where  $\langle \dots \rangle = (1/N) \sum_i (\dots)$  stands for the spatial average. In order to determine  $\tau$  we used the usual relation  $C_{\text{eq}}(\tau) = 1/e$  assuming an exponential decay of the correlations.

Examples of equilibrium correlation functions for different values of the asymmetry parameter  $b$  at the temperature  $T = 0.25$  are shown in figure 1. In the symmetric case, the correlation decays mainly as an exponential (except for long times where the recurrence of defects affects the exponential decay). In the fully asymmetric case a stretched exponential would be better suited. This may affect the determination of the relaxation time and will be discussed later in more detail when studying the persistence functions. In the intermediate case, the correlation starts following the asymmetric case before an exponential behaviour takes place for longer times.

As can be seen in figure 2, the time  $\tau$  agrees with the predicted relaxation time  $\tau_I$ . An Arrhenius law is obtained for the symmetric case. In the fully asymmetric case a quadratic behaviour is seen, but the prefactor  $A = 1/\ln 2$  (see equation (7)) is not exactly recovered. The non-exponential behaviour of the correlations affects the definition of the time  $\tau$  and may explain this discrepancy. Finally, in the intermediate case, the timescale switches from the fragile behaviour to the strong one at the finite temperature  $T_c(b)$ . Notice that below this temperature the timescale can be rescaled by  $b(1-b)$  to remove the  $b$  dependence of the relaxation time  $\tau_I \simeq \tau_S$  (see upper right panel of figure 2).

In the lower right panel of figure 2, we plot the effective energy barrier  $\Delta E = d \ln \tau(T) / d(1/T)$  which displays a linear behaviour for the asymmetric case and gives the expected constant energy barrier  $\Delta E = 1$  for the symmetric case. The crossover from fragile to strong glassy behaviour is more and more pronounced as the asymmetry parameter  $b$  decreases.

<sup>1</sup> We performed numerical simulations using a usual continuous time Monte Carlo algorithm [14] with the Metropolis rule and the dynamical constraints. The system sizes considered ranged from  $10^5$  to  $5 \times 10^6$  spins and the temperatures from  $T = T(b)$  to  $\infty$ , with  $T(b = 0.5) = 0.1$  and  $T(b = 0) = 0.25$ , for the equilibrium simulations. Averages over 10 to 20 runs were performed.

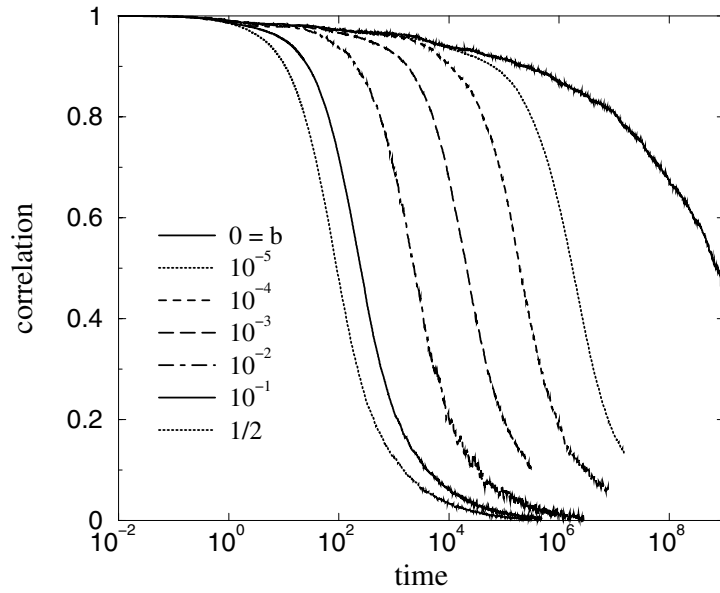


Figure 1. Equilibrium correlation functions for different values of  $b$  at  $T = 0.25$ .

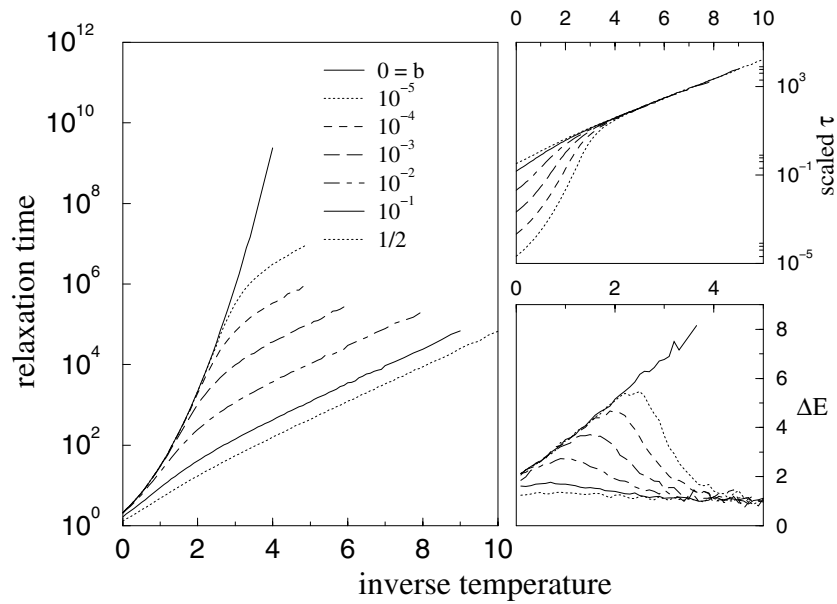


Figure 2. Relaxation time as a function of the inverse temperature  $1/T$  for different values of the asymmetry parameter  $b$  (left). Rescaled relaxation time  $b(1 - b)\tau$  (upper right) and effective energy barrier (lower right) as a function of the inverse temperature.

4.2. Persistence and stretched exponential

The persistence is the fraction of defects present in the initial configuration and which have never flipped up to the time  $t$ :

$$P(t) = c_{\text{eq}}^{-1} \left\langle \prod_{t'=0}^t s_i(t') \right\rangle. \tag{12}$$

This quantity is strongly related to the correlation but is free of the problem of the recurrence of defects which affects the long time behaviour.

In the symmetric case, the persistence may be approximated by the sum of the two possible relaxations of the defects with timescales  $\tau_0$  and  $\tau_1$  corresponding respectively to a defect with and without a neighbouring defect. Assuming those relaxations are exponential

$$P_S(t) \simeq 2c_{\text{eq}}e^{-t/\tau_0} + (1 - 2c_{\text{eq}})e^{-t/\tau_1} \quad (13)$$

where  $2c_{\text{eq}}$  is the probability of a defect having another defect as a neighbour (and neglecting higher orders in  $c_{\text{eq}} \sim e^{-1/T}$ ). The short time behaviour is mainly given by the fastest exponential decay leading to  $-\ln P_S \simeq c_{\text{eq}}t/\tau_0 = t/\tilde{\tau}$  with  $\tilde{\tau} \sim \tau_0 e^{1/T}$  for low temperatures. The long time behaviour is given by  $-\ln P_S \simeq t/\tau_1$ . Both regimes are apparent exponential decays with timescales following an Arrhenius law:  $\tilde{\tau} \sim \tau_1 \sim e^{1/T}$ .

In the asymmetric case, the probability of flipping a defect depends on its distance to the next defect on the right. In equilibrium, the distribution of those lengths is independent of time. The persistence may then be approximated by the sum of the exponential relaxations of the defects with different lengths  $l$

$$P_{\text{AS}}(t) \simeq c_{\text{eq}}e^{-t/\tau_0} + \sum_{k=1}^{\infty} p_k e^{-t/\tau_k} \quad (14)$$

with  $p_k = (1 - c_{\text{eq}})^{2^{k-1}} - (1 - c_{\text{eq}})^{2^k}$  the probability for a defect to have a chain of spins 0 of length  $l$  with  $2^{k-1} \leq l < 2^k$  on its right. Each term in the sum corresponds to a particular energy barrier and timescale. The equilibrium condition is crucial for assuming an independent relaxation of those defects. If this condition is not satisfied, the distribution of lengths evolves in time and the approximation considered is no longer valid.

The small time behaviour is similar to the symmetric case:  $-\ln P(t) \sim t/\tilde{\tau}$ . The long time behaviour may be estimated by replacing the sum by an integral and using a saddle point approximation, following Palmer *et al* [15]. At this point it is interesting to note that the fully asymmetric model falls into one of the classes described in [15]. As a result we obtain a stretched exponential behaviour:

$$P_{\text{AS}}(t) \sim \exp[-(t/\tau_{\text{AS}})^\beta] \quad (t \gg 1) \quad (15)$$

with  $\tau_{\text{AS}}$  the asymmetric relaxation time previously discussed and  $\beta = 1/(1 + 1/T \ln 2)$  the temperature-dependent stretching exponent.

Let us now discuss the intermediate case. At small times the persistence decay is dominated by the asymmetric process due to the entropic barrier for the symmetric one. For really small times the behaviour is analogous to an exponential decay with a timescale  $\tilde{\tau} \sim e^{1/T}$  even though this decay comes mainly from the relaxation process with timescale  $\tau_0 \sim 1$ . The temperature dependence is due to the small prefactor  $c_{\text{eq}} \sim e^{-1/T}$ . At intermediate times we expect a stretched exponential to occur with the stretching exponent  $\beta$ . At large times the symmetric process is dominant and leads to an exponential behaviour with a timescale  $\tau_S(b) \sim e^{1/T + \Delta S}$ .

Figure 3 represents the persistence decay for different temperatures and for two particular asymmetry parameters ( $b = 10^{-3}$  and  $10^{-5}$ ). A double logarithmic scale for the persistence and a logarithmic one for the time have been used to obtain straight lines in the case of stretched exponential behaviour. In both cases the three different regimes are clearly seen and the predicted stretching exponent is observed. The width of the intermediate regime depends on the asymmetry parameter and is larger for smaller  $b$ . The insets show that the small and large time regimes superimpose when the time is rescaled to  $te^{-1/T}$ , as expected.

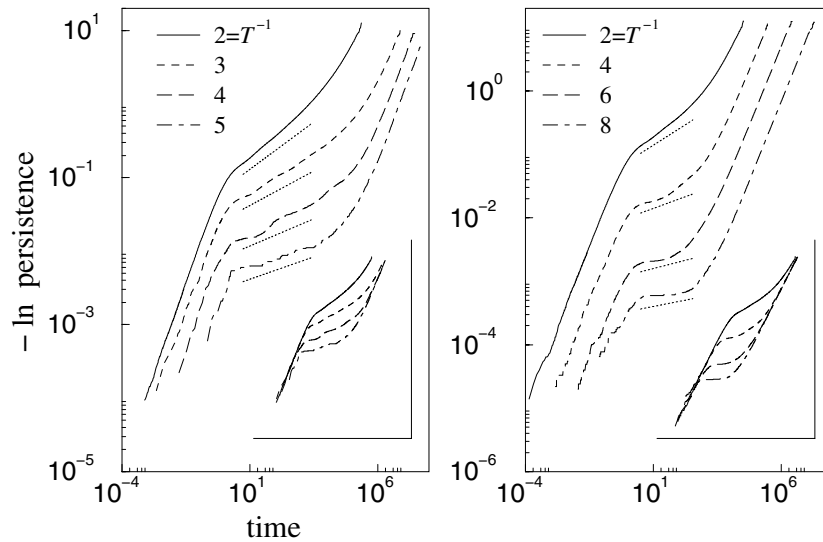


**Figure 3.** Persistence for different temperatures: (left)  $b = 10^{-5}$  and (right)  $b = 10^{-3}$ . Dotted curves are the expected stretching exponents  $\beta$ . Insets: same persistence with a rescaled time  $t' = te^{-1/T}$ .

## 5. Out-of-equilibrium properties

We now discuss some out-of-equilibrium properties. We concentrate on one-time quantities such as the defect concentration. A complete study of two-time quantities like the correlation and the response functions as well as a discussion of the fluctuation dissipation theorem is left to a forthcoming paper.

### 5.1. Defect concentration and plateaux

Starting at  $t = 0$  with an infinite temperature initial configuration and then quenching the system to a low temperature leads to a complicated structure with different plateaux in the decay of the defect concentration towards the equilibrium value. As an example, we plot in figure 4 the defect concentration decay for different asymmetry parameters and a quench temperature  $T = 1/6$ .

In the symmetric case the unique energy barrier leads to a unique plateau. The first decay (up to this first plateau) corresponds to a temperature-independent decay to a configuration where mostly all defects are isolated. The zero-temperature dynamics is independent of the asymmetry parameter and has been solved exactly [6]. The second decay is a diffusion-annihilation process for the defects with a diffusion timescale  $\tau_1 \sim e^{1/T}$  related to the processes described in equations (2) and (3). Thus, this second decay behaves as  $c(t) \sim (t/\tau_1)^{-1/2}$  until the concentration reaches the equilibrium value. The upper dashed line in the inset of figure 4 reflects the  $t^{1/2}$  behaviour of the average distance between defects,  $l(t) = 1/c(t)$ .

In the asymmetric case each energy barrier leads to a plateau due to the corresponding well-separated timescales  $\tau_n \sim e^{n/T}$ . At least four different plateaux are visible in figure 4. The average length behaves as  $t^{T \ln 2}$  as shown by the lower dashed line in the inset of figure 4 [7].

In the intermediate case ( $0 < b < 1/2$ ) the defect concentration follows the curve for the asymmetric case up to  $\tau_S(b) = e^{n^*/T}$  with

$$n^* = 1 + T \Delta S \quad (16)$$



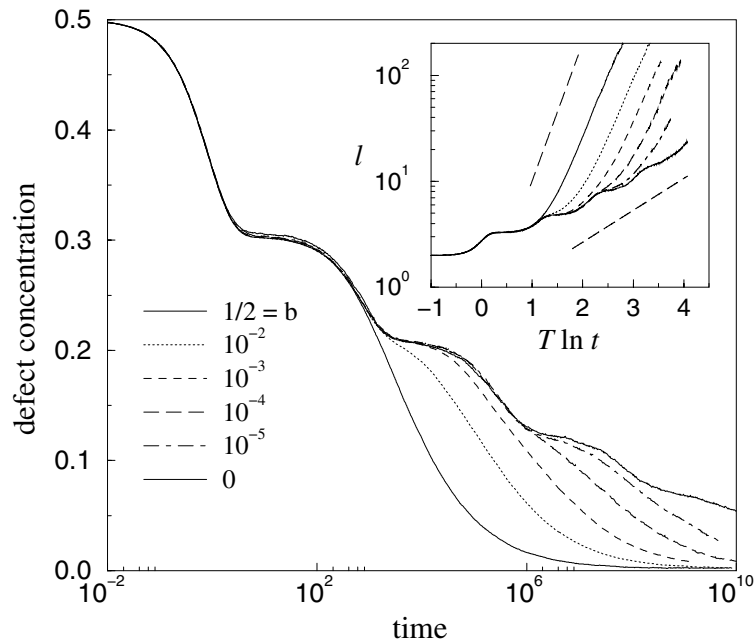


**Figure 4.** Defect concentration as a function of time after a quench from an infinite temperature to a temperature  $T = 1/6$  for different values of the asymmetry parameter  $b$ . Inset: average distance between defects  $l = 1/c$ . The upper dashed line reflects the  $t^{1/2}$  behaviour and the lower dashed line the  $t^{T \ln 2}$  one.

giving the last stage of the asymmetric relaxation that is observed. This value  $n^*$  determines the number of plateaux in the defect concentration decay as a function of the asymmetry parameter. For  $T = 1/6$  we observe the expected number of plateaux in figure 4: three plateaux for  $b = 10^{-5}$  ( $n^* = 2.9$ ), two for  $b = 10^{-4}$  and  $10^{-3}$  ( $n^* = 2.5$  and  $2.2$ ) and only one for  $b = 10^{-2}$  ( $n^* = 1.7$ ).

## 6. Discussion and conclusion

In conclusion we have presented a simple model where the competition between two dynamical processes, one with increasing energy barriers and the other with a unique energy barrier but also an entropic barrier, leads to a crossover from a fragile to strong glassy behaviour as the temperature is lowered (see also [16] for a phenomenological theory). The crossover temperature depends on the tunable entropic barrier. In the fragile regime, a stretched exponential relaxation is predicted with a temperature-dependent stretching exponent.

The entropic barrier is put into this model by hand through an unphysical asymmetry of the dynamical rules. This drawback can be cured in a symmetric model. Let us consider the asymmetry parameter  $b(t)$  as a time-dependent field which takes values  $b = \{0, 1\}$ . The physical origin of this field could be the existence of macro- or mesoscopic regions in the system where new independent variables order (like magnetic moments near the ferromagnetic transition) and influence the dynamical behaviour of the microscopic spins  $s_i$ . Those regions would evolve on a timescale  $\tau_p$ , the simplest example being a Poisson flipping process. With a mean value  $\langle b(t) \rangle = 1/2$  there is no global breaking of the symmetry in the dynamical rules. This argument is then easily generalized to systems in higher dimensions, where the field would be a vector field.

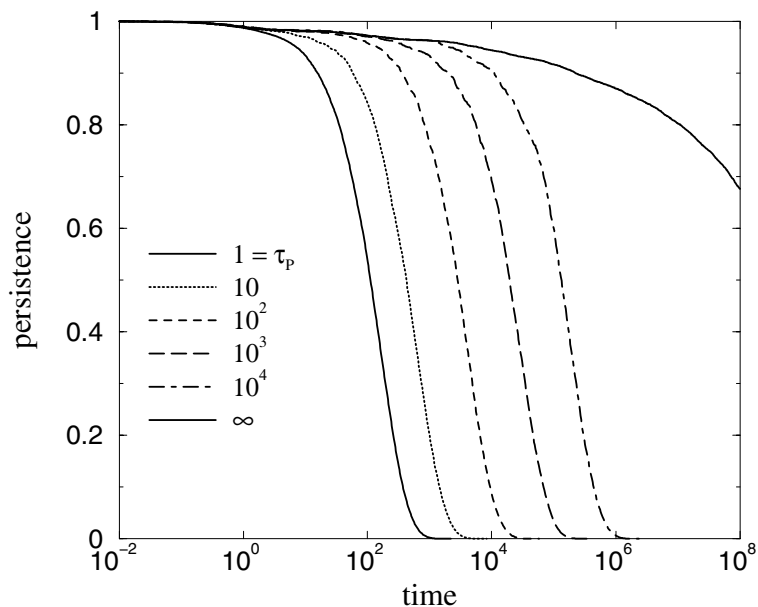


**Figure 5.** Persistence functions for different values of the Poisson timescales  $\tau_p$  at  $T = 0.25$ .

In this new model the system behaves as in the asymmetric case, and thus shows fragile behaviour, on timescales smaller than  $\tau_p$ . On timescales larger than  $\tau_p$ , the asymmetry parameter  $b(t)$  oscillates and the spins only feel the average value  $\langle b(t) \rangle = 1/2$  leading to the symmetric or strong glass behaviour. The timescale  $\tau_p$  replaces the factor  $[b(1-b)]^{-1}$  in the symmetric timescale  $\tau_S(b)$ . The persistence functions plotted in figure 5 show explicitly this crossover from the asymmetric ( $\tau_p = \infty$ ) to the symmetric behaviour for different timescales  $\tau_p$ .

### Acknowledgments

The authors would like to thank David Chandler, Andrea Crisanti, Félix Ritort, Andrea Rocco and Peter Sollich for useful discussions. AB acknowledges financial support from the EU (Marie Curie HPMF-CT-1999-00328) and JPG a Glasstone Research Fellowship (Oxford).

### References

- [1] Angell C A 1995 *Science* **267** 1924
- [2] Sastry S 1999 *Nature* **398** 467
- [3] Ito K, Moynihan C T and Angell C A 1999 *Nature* **398** 492
- [4] Fredrickson G H and Andersen H C 1984 *Phys. Rev. Lett.* **53** 1244
- [5] Jäckle J and Eisinger S 1991 *Z. Phys. B* **84** 115
- [6] Crisanti A, Ritort F, Rocco A and Sellitto M 2001 *J. Chem. Phys.* **113** 10615
- [7] Sollich P and Evans M R 1999 *Phys. Rev. Lett.* **83** 3238
- [8] Schulz M and Trimper S 1999 *J. Stat. Phys.* **94** 173
- [9] Mauch F and Jäckle J 1999 *Physica A* **262** 98
- [10] Buhot A and Garrahan J P 2001 *Phys. Rev. E* **64** 021505
- [11] Bässler H 1987 *Phys. Rev. Lett.* **58** 767
- [12] Vogel R 1921 *Phys. Z.* **22** 645
- [13] Fulcher G S 1925 *J. Am. Ceram. Soc.* **8** 339
- [14] Newman M E J and Barkema G T 1999 *Monte Carlo Methods in Statistical Physics* (Oxford: Oxford University Press)
- [15] Palmer R G, Stein D L, Abrahams E and Anderson P W 1984 *Phys. Rev. Lett.* **53** 958
- [16] Crisanti A and Ritort F 2001 *Preprint cond-mat/0102104*